

Enhanced Superconducting Pairing Strength near a Pure Nematic Quantum Critical Point

Kiyotaka Mukasa^{ⓧ,1}, Kousuke Ishida^{ⓧ,1,*†}, Shusaku Imajo^{ⓧ,2}, Mingwei Qiu,¹ Mikihiro Saito^{ⓧ,1}, Kohei Matsuura,^{1,‡} Yuichi Sugimura^{ⓧ,1}, Supeng Liu^{ⓧ,1}, Yu Uezono,³ Takumi Otsuka,³ Matija Čulo^{ⓧ,4,||}, Shigeru Kasahara,^{5,6} Yuji Matsuda,⁵ Nigel E. Hussey^{ⓧ,4,7}, Takao Watanabe^{ⓧ,3}, Koichi Kindo,² and Takasada Shibauchi^{ⓧ,1,§}

¹Department of Advanced Materials Science, University of Tokyo, Kashiwa, Chiba 277-8561, Japan

²Institute for Solid State Physics, University of Tokyo, Kashiwa, Chiba 277-8581, Japan

³Graduate School of Science and Technology, Hirosaki University, Hirosaki, Aomori 036-8561, Japan

⁴High Field Magnet Laboratory (HFML-EMFL) and Institute for Molecules and Materials, Radboud University, Toernooiveld 7, 6525 ED Nijmegen, Netherlands

⁵Department of Physics, Kyoto University, Kyoto 606-8502, Japan

⁶Research Institute for Interdisciplinary Science, Okayama University, Okayama 700-8530, Japan

⁷H. H. Wills Physics Laboratory, University of Bristol, Tyndall Avenue, Bristol BS8 1TL, United Kingdom



(Received 21 March 2022; revised 23 September 2022; accepted 31 January 2023; published 6 March 2023)

The quest for high-temperature superconductivity at ambient pressure is a central issue in physics. In this regard, the relationship between unconventional superconductivity and the quantum critical point (QCP) associated with the suppression of some form of symmetry-breaking order to zero temperature has received particular attention. The key question is how the strength of the electron pairs changes near the QCP, and this can be verified by high-field experiments. However, such studies are limited mainly to superconductors with magnetic QCPs, and the possibility of unconventional mechanisms by which nonmagnetic QCP promotes strong pairing remains a nontrivial issue. Here, we report systematic measurements of the upper critical field H_{c2} in nonmagnetic $\text{FeSe}_{1-x}\text{Te}_x$ superconductors, which exhibit a pure QCP of electronic nematicity characterized by spontaneous rotational-symmetry breaking. As the magnetic field increases, the superconducting phase of $\text{FeSe}_{1-x}\text{Te}_x$ shrinks to a narrower dome surrounding the nematic QCP. The analysis of H_{c2} reveals that the Pauli-limiting field is enhanced toward the QCP, implying that the pairing interaction is significantly strengthened via nematic fluctuations emanating from the QCP. Remarkably, this nematic QCP is not accompanied by a divergent effective mass, distinct from the magnetically mediated pairing. Our observation opens up a nematic route to high-temperature superconductivity.

DOI: 10.1103/PhysRevX.13.011032

Subject Areas: Condensed Matter Physics,
Strongly Correlated Materials,
Superconductivity

I. INTRODUCTION

Unconventional superconductors, whose mechanisms of electron pairing are distinct from the conventional electron-phonon interaction, have been a focus of

interest in condensed matter physics. It has been increasingly recognized that most of their parent materials undergo a phase transition into some form of long-range electronic order. The superconducting transition temperature T_c often reaches a maximum at a quantum critical point (QCP), where a continuous order-disorder transition of coexisting order takes place at absolute zero temperature. This implies that quantum fluctuations intensified at the QCP might strengthen the interaction binding Cooper pairs, leading to an enhanced magnitude of the superconducting gap. Mapping out the upper critical field H_{c2} , especially the Pauli-limiting field which is a fundamental measure of the superconducting condensation energy [1,2], across the superconducting phase diagram is a direct test for the impact of a QCP on superconductivity. However, in many cases, H_{c2} is governed by the orbital pair-breaking effect, and it often requires a very high magnetic field, which makes such evaluations difficult.

*Present address: Max Planck Institute for Chemical Physics of Solids, Nöthnitzer Straße 40, 01187 Dresden, Germany.

†kousuke.ishida@cpfs.mpg.de

‡Present address: Department of Applied Physics, University of Tokyo, Bunkyo-ku, Tokyo 113-8656, Japan.

||Present address: Institut za fiziku, P.O. Box 304, HR-10001 Zagreb, Croatia.

§shibauchi@k.u-tokyo.ac.jp

Published by the American Physical Society under the terms of the Creative Commons Attribution 4.0 International license. Further distribution of this work must maintain attribution to the author(s) and the published article's title, journal citation, and DOI.

While an increase of T_c has been often observed near the QCP of antiferromagnetic order [3,4], electronic nematicity, which breaks a rotational symmetry of the underlying lattice while preserving a translational symmetry, has been found in several classes of unconventional superconductors including high- T_c copper oxides [5,6], heavy-fermion compounds [7,8], and iron-based superconductors [9,10]. Although it has been theoretically proposed that nematic fluctuations can have a cooperative relation to superconductivity [11–13], the enhancement of T_c associated with the nematic QCP in these compounds is still under debate. This is mostly because the electronic nematic orders found in the correlated systems often intertwine with other charge or spin degrees of freedom (charge- [14] or spin- [10] density waves), and they do not exist in isolation.

In this context, the iron-chalcogenide superconductor FeSe is an important material [15–17]. Below $T_s \approx 90$ K, FeSe exhibits a unique nematic order, which does not accompany long-range magnetic order, unlike other iron-based superconductors [18]. This pure nematic order can be controlled by physical pressure [19] as well as by isovalent substitution of S for Se sites [20]. In both cases, however, there is no evidence for T_c enhancement associated with the QCP of the nematic phase. In the temperature versus pressure phase diagrams of FeSe $_{1-x}$ S $_x$ [21], T_c is less affected by the nematic end point, while T_c increases above 30 K at the point where the pressure-induced magnetic order disappears. At ambient pressure, T_c of FeSe $_{1-x}$ S $_x$ shows a broad maximum at $x \approx 0.10$ inside the nematic phase but decreases to approximately 4 K above the nematic QCP at $x_c \approx 0.17$ [22]. Nuclear-magnetic-resonance (NMR) measurements reveal a correlation between T_c and the strength of spin-lattice relaxation rate $1/T_1T$ inside the nematic phase, suggesting the importance of spin fluctuations despite the absence of long-range magnetic order in FeSe $_{1-x}$ S $_x$ [23].

Recently, in contrast to the S substitution and physical pressure cases, FeSe $_{1-x}$ Te $_x$ has been found to show an enhancement of T_c near the end point of the nematic phase at $x_c \approx 0.50$ without static magnetism [24,25]. With Te substitution, T_c first decreases to its local minimum at $x \approx 0.30$ and then turns to increase toward a broad maximum at $x \approx 0.60$ with $T_c \approx 14$ K. The electron-phonon-coupling strength, as estimated by Raman spectroscopy [26], is far too small to explain the observed T_c value, pointing to an unconventional origin of the electron pairing. Elastoresistivity studies have shown that the nematic susceptibility of FeSe $_{1-x}$ Te $_x$ follows a Curie-Weiss temperature dependence over a wide region of the phase diagram, evidencing the presence of a nonmagnetic nematic QCP [27–29]. Moreover, the superconducting dome of FeSe $_{1-x}$ Te $_x$ straddles the nematic QCP, making it the first viable example of a system exhibiting a link between pure nematic fluctuations and enhanced superconductivity. To verify the notion of electron pairing

promoted by nematic fluctuations, however, it is essential to clarify how the pairing strength evolves in the phase diagram. In this study, we present systematic studies of superconductivity in FeSe-based materials at high magnetic fields up to 60 T. Thanks to their modest T_c , we succeed in completely suppressing the superconducting phase across the entire phase diagram.

II. METHODS

Single crystals of FeSe $_{1-x}$ S $_x$ and FeSe $_{1-x}$ Te $_x$ for $0 < x \leq 0.48$ are grown by the chemical-vapor-transport (CVT) technique [24]. Single crystals of FeSe $_{1-x}$ Te $_x$ for $0.52 \leq x \leq 0.90$ are obtained by the Bridgman method [30]. For the crystals synthesized by the Bridgman method, the Te annealing procedure is applied to minimize the excess Fe [30], which is known to be crucial to evaluate the intrinsic physical properties of FeSe $_{1-x}$ Te $_x$ [31]. The actual Te composition x of FeSe $_{1-x}$ Te $_x$ synthesized by the CVT method is determined for each sample from the c -axis length measured by x-ray diffraction measurements. The x values of crystals grown by the Bridgman method are taken from the nominal values.

High-field electrical resistance and tunnel-diode-oscillator (TDO) measurements of FeSe $_{1-x}$ Te $_x$ are carried out at the International MegaGauss Science Laboratory, Institute for Solid State Physics in University of Tokyo, using a 60-T pulsed magnet. In the TDO measurements, a TDO circuit with a 0.7-mm-diameter 8-shaped copper coil (approximately eight turns to cancel out the induction voltage of the pulsed magnetic fields) is operated at approximately 82 MHz. We also perform complementary measurements of the electrical resistance of FeSe $_{1-x}$ Te $_x$ under low magnetic fields up to 7 T in a physical-property-measurement system (Quantum Design). Magnetoresistance measurements of FeSe $_{1-x}$ S $_x$ are performed at the High Field Magnet Laboratory in Nijmegen. For the electrical-resistance measurements, we use the conventional four-terminal method with current applied within the $a - b$ plane. The electrical contacts are made using gold wires. For FeSe $_{1-x}$ Te $_x$, the contacts are first made by gold paste (SILBEST no. 8560, Tokuriki Chemical Research), which can give a good contact resistance less than a few ohms to iron chalcogenides, and then covered by silver paste (DuPont 4922) to fix them more firmly. The typical sample size of FeSe $_{1-x}$ Te $_x$ is approximately $1 \times 0.5 \times 0.03$ mm³, and excitation currents are 1–3 mA. In all the measurements, the magnetic field is applied along the c axis.

III. RESULTS

Figure 1 presents the transverse magnetoresistance data for $x = 0.11$ (a), 0.48 (b), and 0.80 (c). As x increases, the orbital magnetoresistance in the normal state gradually weakens, and its slope changes from positive to negative (see Supplemental Material [32] for all the

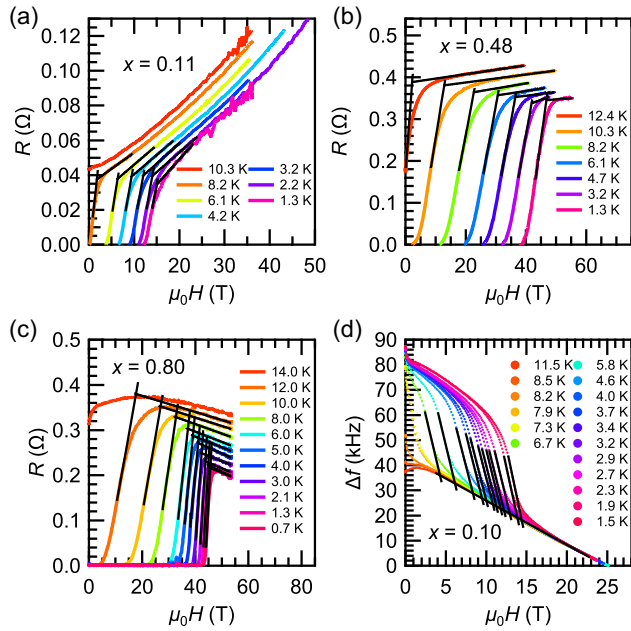


FIG. 1. Determination of H_{c2} in $\text{FeSe}_{1-x}\text{Te}_x$. (a)–(c) Magneto-resistance measured at several temperatures for $x = 0.11$ (a), 0.48 (b), and 0.80 (c). The upper critical field H_{c2} is defined as an intersection of the two black lines. (d) Magnetic field dependence of the change in the resonant frequency Δf observed in the TDO measurement for $x = 0.10$. H_{c2} is determined from the point where two black lines are crossing.

magneto-resistance data). In order to determine the upper critical fields H_{c2} for all the compositions regardless of the sign of magneto-resistance, we define H_{c2} as the field where two lines extrapolated from the resistance curves in the flux-flow regime and normal state intersect [black lines in Figs. 1(a)–1(c)]. Radio-frequency penetration-depth measurements using a TDO are performed for four low- x compositions to confirm the consistency of H_{c2} values with that obtained from the magneto-resistance data since these compositions show noticeable orbital magneto-resistances, which might affect the fitting analysis of the normal-state resistance (procedure 1 presented in the Supplemental Material [32] “Upper critical field estimated from magneto-resistance data”). The shift in the resonant frequency of the TDO circuit Δf is proportional to the magnetic penetration depth. As shown in the field dependence of Δf for $x = 0.10$ displayed in Fig. 1(d), a clear signature of the superconducting transition is observed, and H_{c2} is determined from an intersection of two extrapolated lines (see Supplemental Material [32] for TDO data in the other three compositions). The obtained temperature dependence of $H_{c2}(T)$ for the representative Te compositions is shown in Fig. 2 (see Supplemental Material [32] for all compositions). The $H_{c2}(T)$ data determined from the magneto-resistance for $x = 0.11$ and from TDO measurements for $x = 0.10$ almost coincide with each other [Fig. 2(a)], confirming that our estimates of H_{c2} are reasonable. In a

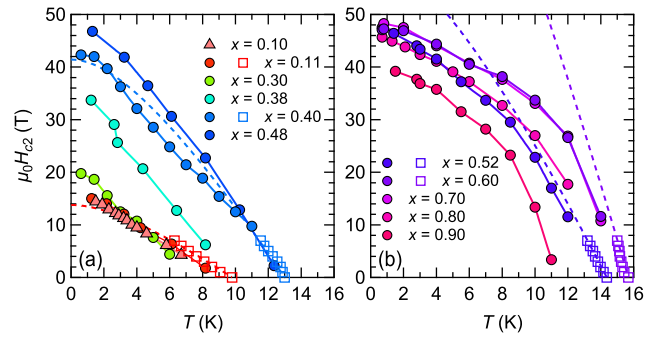


FIG. 2. Temperature dependence of the upper critical field H_{c2} in $\text{FeSe}_{1-x}\text{Te}_x$. (a),(b) $H_{c2}(T)$ for the compositions (a) inside and (b) outside of nematic phase determined from the TDO (triangles) and the resistance (circles) measurements under pulsed high magnetic fields. Solid lines represent the linear interpolation between each datum. Dashed lines show fits to the low-field data (open squares) measured under the steady field up to 7 T within the Helfand-Werthamer framework, which includes only the orbital pair-breaking effect.

wide composition range between $x = 0.48$ and 0.70, the H_{c2} values at the lowest temperature are essentially unchanged at 46–48 T, in good agreement with the previous reports for $x = 0.52$ [33] and $x = 0.60$ [34].

From the linear interpolation of the $H_{c2}(T)$ data, we obtain the T_c values at several magnetic field strengths H . In Fig. 3, we show how the magnetic field changes the superconducting phases of $\text{FeSe}_{1-x}\text{Te}_x$. Remarkably, at $\mu_0 H = 14$ T, T_c for $x < 0.30$ is strongly suppressed, as a

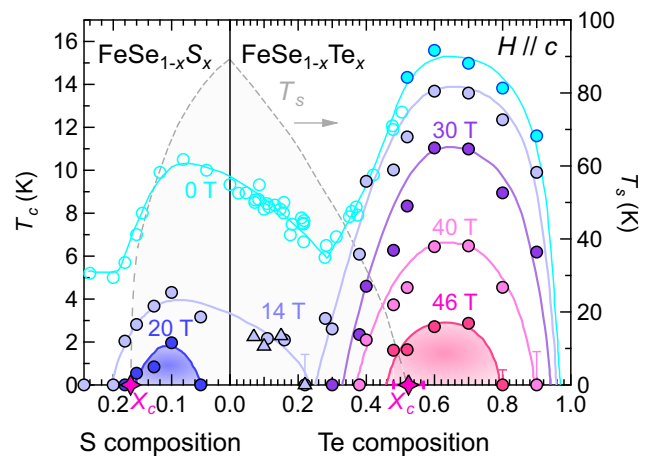


FIG. 3. Field-induced change of superconducting phases in FeSe -based superconductors. T_c values at finite fields are determined from the temperature dependence of H_{c2} measured by magneto-resistance (closed circles) and TDO technique (triangles). T_c values at zero field shown by open circles are taken from the data previously measured in the single crystals grown by the CVT technique [24]. Zero-temperature intercepts of the structural transition T_s shown by the gray dashed line represent the nematic quantum critical points x_c . All the solid lines are guides to the eye.

result of which the superconducting phase splits into two separated regions. Combining the T_c values of $\text{FeSe}_{1-x}\text{S}_x$ obtained by applying the same analysis protocol to its magnetoresistance data [35,36], we find that at $\mu_0 H = 14$ T, FeSe exhibits two distinct superconducting domes as a function of the chemical pressure applied by isovalent substitution. At $\mu_0 H = 30$ T, the superconductivity completely disappears at $x < 0.30$ of $\text{FeSe}_{1-x}\text{Te}_x$, leaving a single superconducting dome centered at $x = 0.60$. Moreover, as the magnetic field further increases to $\mu_0 H = 40$ and 46 T, this dome shrinks to a narrower x region straddling the nematic QCP ($x_c \approx 0.50$). It should be noted that at $\mu_0 H = 46$ T, while the superconductivity for $x = 0.80$ is considerably suppressed to below 0.7 K, T_c for $x = 0.48$ and 0.52 closer to nematic QCP remains around 1.6 K. This suggests an intimate relationship between the nematic QCP and the superconducting dome in $\text{FeSe}_{1-x}\text{Te}_x$. These are the main findings of the present paper.

IV. DISCUSSION

The observation of two disconnected superconducting domes, which shrink in a different manner in the presence of a magnetic field, hints at distinct superconducting phases. The positions of the dome centers provide valuable clues as to their origin. In the lower dome peaked around $x \approx 0.10$ in $\text{FeSe}_{1-x}\text{S}_x$, magnetic fluctuations are likely to play a dominant role since the nematic QCP of $\text{FeSe}_{1-x}\text{S}_x$ is pushed outside the dome at 20 T while several probes have detected substantial stripe-type antiferromagnetic spin fluctuations inside the nematic phase [23,37]. In $\text{FeSe}_{1-x}\text{Te}_x$ by contrast, the spin-lattice relaxation rate $1/T_1 T$ obtained from NMR is shown to be temperature independent for $x = 0.58$ indicating the absence of strong spin fluctuations near the higher dome [38]. The double-stripe magnetism, whose magnetic structure is different from that discussed in $\text{FeSe}_{1-x}\text{S}_x$, is known to appear in $\text{FeSe}_{1-x}\text{Te}_x$. However, the properly annealed crystals show this magnetic order in a very narrow region with $x > 0.92$ [30], and a neutron scattering study has revealed that it is rather destructive to the superconductivity [39]. Although the detailed Te composition dependence of spin fluctuations between $x = 0$ and $x \approx 0.50$ is currently lacking, the pressure-induced magnetic order found in the region including the lower T_c dome has been found to disappear below 8 GPa for $x \geq 0.14$ of $\text{FeSe}_{1-x}\text{Te}_x$ [24], suggesting that magnetic interactions become weaker in the higher- T_c dome region. Furthermore, nematic fluctuations are expected to be insensitive in this range of magnetic field, as reported by recent elastoresistivity measurements on the electron-doped iron pnictides showing that the nematic susceptibility does not have a significant field dependence up to 65 T [40]. Therefore, our observation suggests that nematic fluctuations are likely more responsible for the field-robust superconducting dome in $\text{FeSe}_{1-x}\text{Te}_x$.

Of course, one may contemplate an alternative scenario in which there is a single pairing mechanism underlying each dome with T_c depending solely on the density of states participating in the formation of Cooper pairs or the effect of multiband superconducting-gap structure. However, such a scenario would have to be reconciled with the contrasting strength of nematic and magnetic fluctuations across the two domes. Moreover, scanning tunneling spectroscopy revealed that optimally substituted $\text{FeSe}_{1-x}\text{Te}_x$ shows a full-gap superconductivity [41] while superconducting-gap structures of $\text{FeSe}_{1-x}\text{S}_x$ are highly anisotropic [42], supporting the scenario of distinct pairing mechanisms within the two domes. Our observation should motivate additional experiments to unequivocally rule out other possibilities.

More detailed analysis of the upper critical fields can provide us with more direct insights into the close relationship between the nematic QCP and pairing strength in $\text{FeSe}_{1-x}\text{Te}_x$. It has been argued that $H_{c2}(T)$ of FeSe and $\text{FeSe}_{1-x}\text{Te}_x$ with $x \approx 0.50$ –0.70 shows Pauli-limited behavior at low temperatures [33,34,43]. In Fig. 2, we compare the measured values with the curves extrapolated from the low-field data (open squares) using the Helfand-Werthamer (HW) formalism, which can yield $H_{c2}(T)$ assuming only the effect of orbital depairing [44]. For $x < 0.40$, there is no strong downward deviation from the HW fitting curves at low temperatures. One possible reason for this unexpected behavior is that the resistivity measurements tend to underestimate the initial slope of H_{c2} with respect to that thermodynamically determined from, e.g., heat capacity measurements [45]. In contrast, for $x > 0.50$ outside the nematic phase, HW curves clearly go beyond the measured values, indicating a significant paramagnetic pair-breaking effect. This is consistent with the nearly isotropic H_{c2} at $x = 0.67$ [43], whereas the orbital-depairing effect should reflect the anisotropic quasi-two-dimensional electronic structure of $\text{FeSe}_{1-x}\text{Te}_x$. In this composition range, where the orbital critical field $H_{\text{orb}}(0)$ exceeds $H_{c2}(0)$, the Pauli-limited field $H_{\text{Pauli}}(0)$ can be estimated using the expression [46]

$$H_{\text{Pauli}}(0) = \frac{\sqrt{2}H_{\text{orb}}(0)}{\sqrt{[H_{\text{orb}}(0)/H_{c2}(0)]^2 - 1}} \quad (1)$$

in which the contribution from spin-orbit coupling is neglected. Using the measured $H_{c2}(0)$ values and the orbital critical field derived from $H_{\text{orb}}(0) = -0.69T_c \times dH_{c2}/dT|_{T_c}$ (see Supplemental Material [32]), we plot the x dependence of the obtained Pauli-limited field H_{Pauli} in Fig. 4. The value of $H_{\text{Pauli}}(0)$ is known to be connected to the magnitude of the zero-temperature superconducting gap Δ_0 as $\sqrt{2}\Delta_0 = g\mu_B\mu_0 H_{\text{Pauli}}(0)$, where g and μ_B are the g factor and the Bohr magneton, respectively. For all compositions, $\mu_0 H_{\text{Pauli}}/T_c \propto \Delta_0/T_c$ —a measure of the pairing strength—is well above $\mu_0 H_{\text{Pauli}}(0)/T_c = 1.84$ T/K, the

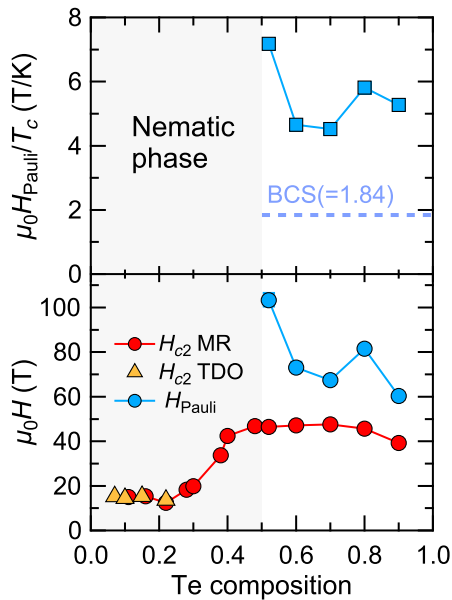


FIG. 4. Te composition x dependence of the upper critical field in $\text{FeSe}_{1-x}\text{Te}_x$. The bottom panel displays H_{c2} at the lowest temperature determined by the resistance (red circles) and TDO (yellow triangles) measurements, and the Pauli-limited field H_{Pauli} (blue circles) estimated as mentioned in the main text. The top panel shows H_{Pauli} (blue squares) divided by their critical temperature T_c . The dashed line indicates the value predicted in weak-coupling BCS theory. The gray shades represent the compositions where nematic phase appears.

value expected for a weak-coupling BCS superconductor, as shown in Fig. 4. This demonstrates that superconductivity in $\text{FeSe}_{1-x}\text{Te}_x$ lies in the strong-coupling regime, as discussed previously in the context of the BCS-BEC crossover [47]. More importantly, we find that $\mu_0 H_{\text{Pauli}}/T_c$ becomes largest at $x = 0.52$. Although this analysis cannot be applied to data inside the nematic phase, it clearly indicates that the electron pairing is strengthened upon approach to the nematic QCP in the tetragonal phase.

It is noteworthy that the broad $T_c(x)$ dome near the nematic QCP of $\text{FeSe}_{1-x}\text{Te}_x$ is widened to the high-Te substitution side. One possibility related to this point is that the actual QCP beneath the superconducting dome locates at a composition higher than the end point of the $T_s(x)$ line extrapolated from the normal state. A recent theory has pointed out that since the nematic phase of iron chalcogenides is cooperative to the superconductivity, as demonstrated by the increase of orthorhombicity below T_c [48], the $T_s(x)$ line would show a forward bending when it meets the superconducting transition line [49]. This predicted behavior is opposite to the back bending of the $T_s(x)$ line below T_c observed in $\text{Ba}(\text{Fe}_{1-x}\text{Co}_x)_2\text{As}_2$ [50], where the sharp hardening of elastic constants below T_c has clearly shown the competing relation between nematicity and superconductivity [51]. Another possible origin is an increasing trend of the density of states toward FeTe

associated with the orbital-selective mass renormalization featuring the strongest correlations in the d_{xy} -dominated bands [52]. Moreover, our analysis of the Pauli-limited field indicates that the enhanced pairing interactions near the QCP would cause a pair-breaking effect, which results in a slight suppression of T_c while maintaining a large Δ_0 . Although the spin fluctuations are shown to have such a pair-breaking effect [53], the case of nonmagnetic nematic fluctuations is less clear and deserves further investigation.

It is expected that the bosonic interaction strengthening Cooper pairing, which likely corresponds to nematic fluctuations in $\text{FeSe}_{1-x}\text{Te}_x$, can also lead to a strong renormalization of the quasiparticle effective mass m^* . In $\text{BaFe}_2(\text{As},\text{P})_2$, several probes indicate a diverging m^* toward the antiferromagnetic QCP, where critical spin fluctuations promote T_c [3]. However, in nonmagnetic $\text{FeSe}_{1-x}\text{Te}_x$ an earlier angle-resolved photoemission-spectroscopy study has shown that although the dispersions are strongly renormalized over all the Te compositions compared to those in $\text{BaFe}_2(\text{As},\text{P})_2$, there are no signatures of mass enhancement in the vicinity of the nematic QCP in any of the orbitals located around the Γ point [54], consistent with the lack of an enhancement in $H_{\text{orb}}(0)$ toward the QCP (see Supplemental Material [32]). This absence of any strong enhancement in the effective mass might be related to the nematoelastic-coupling effect, which restricts the divergence of the correlation length at the nematic QCP only along high-symmetry directions [55]. In $\text{FeSe}_{1-x}\text{S}_x$, in which the nematoelastic coupling has been estimated to be close to that in $\text{FeSe}_{1-x}\text{Te}_x$ [27], a quantum oscillation study found no evidence of mass enhancement near the nematic QCP [56], although non-trivial departures from Fermi liquid behavior in the magnetotransport have been observed near the QCP [57–59]. On the other hand, it is pointed out that the strong nematoelastic coupling allows the system to be treated within the weak-coupling regime, which contrasts with our observations of strong coupling in $\text{FeSe}_{1-x}\text{Te}_x$ [60]. Whatever the mechanism of its absence is, an enhanced pairing strength in the vicinity of the nematic QCP in $\text{FeSe}_{1-x}\text{Te}_x$ without accompanying apparent mass divergence clearly suggests that nematic and antiferromagnetic fluctuations promote Cooper pairing by a fundamentally different mechanism. Together with the field-robust superconducting dome around the nematic QCP, our results imply that $\text{FeSe}_{1-x}\text{Te}_x$ could be an ideal playground in which to study in depth the underlying physics of superconductivity enhanced by nematic critical fluctuations.

Isovalent substitution is recognized as a relatively clean tuning parameter in iron-based superconductors due to the fact that it replaces elements outside of the Fe layers. One intriguing aspect of our observation is that although the electronic structure in the isovalently substituted FeSe maintains electron-hole compensation without introducing

strong disorder, the phase diagram displays two distinct superconducting phases. Two distinct T_c domes have been also found in the phase diagrams of high- T_c cuprates [61–63] and heavy fermion compound CeCu_2Si_2 [64]. In these systems, just as in the FeSe-based system considered here, one dome is connected to antiferromagnetic fluctuations while the other is likely to be associated with fluctuations of nonmagnetic order—the valence transition in CeCu_2Si_2 and the electronic nematic order in $\text{FeSe}_{1-x}\text{Te}_x$. As for the cuprates, while there exists significant evidence that charge order strongly competes with superconductivity [65–67], which forms the two- T_c -dome structure, effective mass enhancement toward the center of a higher- T_c dome observed in a quantum oscillation study [62] would be related to a QCP of nonmagnetic origin. This might be highlighting the delicate balance of the interactions between spin and other degrees of freedom in these correlated electron systems, and the dominant fluctuations that finally lead to the formation of Cooper pairing.

ACKNOWLEDGMENTS

We thank S. A. Kivelson, Y. Mizukami, H. Kontani, and I. Paul for the fruitful discussion and J. Ayres, J. Buhot, and S. Licciardello for assistance with the Fe(Se,S) high-field data. This work was partially carried out by the joint research in the Institute for Solid State Physics, University of Tokyo and HFML-RU/NWO, a member of the European Magnetic Field Laboratory (EMFL). This work was supported by Grants-in-Aid for Scientific Research (KAKENHI Grants No. JP22H00105, No. JP20K03849, No. JP19H00649, and No. JP18H05227), Grant-in-Aid for Scientific Research on Innovative Areas “Quantum Liquid Crystals” (KAKENHI Grant No. JP19H05824) from the Japan Society for the Promotion of Science, and by JST CREST (Grant No. JPMJCR19T5). N. E. H. and M. C. acknowledge support from the Netherlands Organisation for Scientific Research (Grant No. 16METL01) “Strange Metals” and the European Research Council under the European Union’s Horizon 2020 research and innovation program (Grant Agreement No. 835279-Catch-22). N. E. H. also acknowledges the support of EPSRC (Grant ref. EP/V02986X/1). The work at Hirosaki was supported by Hirosaki University Grant for Distinguished Researchers from fiscal year 2017 to 2018.

K. M. and K. I. contributed equally to this work.

-
- [1] A. M. Clogston, *Upper Limit for the Critical Field in Hard Superconductors*, *Phys. Rev. Lett.* **9**, 266 (1962).
 [2] B. S. Chandrasekhar, *A Note on the Maximum Critical Field of High-Field Superconductors*, *Appl. Phys. Lett.* **1**, 7 (1962).
 [3] T. Shibauchi, A. Carrington, and Y. Matsuda, *A Quantum Critical Point Lying Beneath the Superconducting Dome in*

- Iron Pnictides*, *Annu. Rev. Condens. Matter Phys.* **5**, 113 (2014).
 [4] N. D. Mathur, F. M. Grosche, S. R. Julian, I. R. Walker, D. M. Freye, R. K. W. Haselwimmer, and G. G. Lonzarich, *Magnetically Mediated Superconductivity in Heavy Fermion Compounds*, *Nature (London)* **394**, 39 (1998).
 [5] Y. Sato, S. Kasahara, H. Murayama, Y. Kasahara, E. G. Moon, T. Nishizaki, T. Loew, J. Porras, B. Keimer, T. Shibauchi, and Y. Matsuda, *Thermodynamic Evidence for a Nematic Phase Transition at the Onset of the Pseudogap in $\text{YBa}_2\text{Cu}_3\text{O}_y$* , *Nat. Phys.* **13**, 1074 (2017).
 [6] K. Ishida, S. Hosoi, Y. Teramoto, T. Usui, Y. Mizukami, K. Itaka, Y. Matsuda, T. Watanabe, and T. Shibauchi, *Divergent Nematic Susceptibility near the Pseudogap Critical Point in a Cuprate Superconductor*, *J. Phys. Soc. Jpn.* **89**, 064707 (2020).
 [7] R. Okazaki, T. Shibauchi, H. J. Shi, Y. Haga, T. D. Matsuda, E. Yamamoto, Y. Onuki, H. Ikeda, and Y. Matsuda, *Rotational Symmetry Breaking in the Hidden-Order Phase of URu_2Si_2* , *Science* **331**, 439 (2011).
 [8] F. Ronning, T. Helm, K. R. Shirer, M. D. Bachmann, L. Balicas, M. K. Chan, B. J. Ramshaw, R. D. McDonald, F. F. Balakirev, M. Jaime, E. D. Bauer, and P. J. Moll, *Electronic In-Plane Symmetry Breaking at Field-Tuned Quantum Criticality in CeRhIn_5* , *Nature (London)* **548**, 313 (2017).
 [9] R. M. Fernandes, A. V. Chubukov, and J. Schmalian, *What Drives Nematic Order in Iron-Based Superconductors?*, *Nat. Phys.* **10**, 97 (2014).
 [10] J.-H. Chu, H.-H. Kuo, J. G. Analytis, and I. R. Fisher, *Divergent Nematic Susceptibility in an Iron Arsenide Superconductor*, *Science* **337**, 710 (2012).
 [11] H. Kontani and S. Onari, *Orbital-Fluctuation-Mediated Superconductivity in Iron Pnictides: Analysis of the Five-Orbital Hubbard-Holstein Model*, *Phys. Rev. Lett.* **104**, 157001 (2010).
 [12] S. Lederer, Y. Schattner, E. Berg, and S. A. Kivelson, *Enhancement of Superconductivity near a Nematic Quantum Critical Point*, *Phys. Rev. Lett.* **114**, 097001 (2015).
 [13] S. Lederer, Y. Schattner, E. Berg, and S. A. Kivelson, *Superconductivity and Non-Fermi Liquid Behavior near a Nematic Quantum Critical Point*, *Proc. Natl. Acad. Sci. U.S.A.* **114**, 4905 (2017).
 [14] C. Eckberg, D. J. Campbell, T. Metz, J. Collini, H. Hodovanets, T. Drye, P. Zavalij, M. H. Christensen, R. M. Fernandes, S. Lee, P. Abbamonte, J. W. Lynn, and J. Paglione, *Sixfold Enhancement of Superconductivity in a Tunable Electronic Nematic System*, *Nat. Phys.* **16**, 346 (2020).
 [15] T. Shibauchi, T. Hanaguri, and Y. Matsuda, *Exotic Superconducting States in FeSe-Based Materials*, *J. Phys. Soc. Jpn.* **89**, 102002 (2020).
 [16] A. Kreisel, P. J. Hirschfeld, and B. M. Andersen, *On the Remarkable Superconductivity of FeSe and Its Close Cousins*, *Symmetry* **12**, 1402 (2020).
 [17] A. I. Coldea, *Electronic Nematic States Tuned by Isoelectronic Substitution in Bulk $\text{FeSe}_{1-x}\text{S}_x$* , *Front. Phys.* **8**, 594500 (2021).
 [18] A. E. Böhmer, F. Hardy, F. Eilers, D. Ernst, P. Adelman, P. Schweiss, T. Wolf, and C. Meingast, *Lack of Coupling between Superconductivity and Orthorhombic Distortion in*

- Stoichiometric Single-Crystalline FeSe*, *Phys. Rev. B* **87**, 180505(R) (2013).
- [19] J.P. Sun, K. Matsuura, G.Z. Ye, Y. Mizukami, M. Shimozawa, K. Matsubayashi, M. Yamashita, T. Watashige, S. Kasahara, Y. Matsuda, J.Q. Yan, B.C. Sales, Y. Uwatoko, J.G. Cheng, and T. Shibauchi, *Dome-Shaped Magnetic Order Competing with High-Temperature Superconductivity at High Pressures in FeSe*, *Nat. Commun.* **7**, 12146 (2016).
- [20] S. Hosoi, K. Matsuura, K. Ishida, H. Wang, Y. Mizukami, T. Watashige, S. Kasahara, Y. Matsuda, and T. Shibauchi, *Nematic Quantum Critical Point without Magnetism in FeSe_{1-x}S_x Superconductors*, *Proc. Natl. Acad. Sci. U.S.A.* **113**, 8139 (2016).
- [21] K. Matsuura *et al.*, *Maximizing T_c by Tuning Nematicity and Magnetism in FeSe_{1-x}S_x Superconductors*, *Nat. Commun.* **8**, 1143 (2017).
- [22] Y. Mizukami, M. Haze, O. Tanaka, K. Matsuura, D. Sano, J. Böker, I. Eremin, S. Kasahara, Y. Matsuda, and T. Shibauchi, *Thermodynamics of Transition to BCS-BEC Crossover Superconductivity in FeSe_{1-x}S_x*, *arXiv:2105.00739*.
- [23] P. Wiecki, K. Rana, A. E. Böhmer, Y. Lee, S. L. Bud'ko, P. C. Canfield, and Y. Furukawa, *Persistent Correlation between Superconductivity and Antiferromagnetic Fluctuations near a Nematic Quantum Critical Point in FeSe_{1-x}S_x*, *Phys. Rev. B* **98**, 020507(R) (2018).
- [24] K. Mukasa, K. Matsuura, M. Qiu, M. Saito, Y. Sugimura, K. Ishida, M. Otani, Y. Onishi, Y. Mizukami, K. Hashimoto, J. Gouchi, R. Kumai, Y. Uwatoko, and T. Shibauchi, *High-Pressure Phase Diagrams of FeSe_{1-x}Te_x: Correlation between Suppressed Nematicity and Enhanced Superconductivity*, *Nat. Commun.* **12**, 381 (2021).
- [25] K. Terao, T. Kashiwagi, T. Shizu, R. A. Klemm, and K. Kadowaki, *Superconducting and Tetragonal-to-Orthorhombic Transitions in Single Crystals of FeSe_{1-x}Te_x (0 ≤ x ≤ 0.61)*, *Phys. Rev. B* **100**, 224516 (2019).
- [26] S.-F. Wu, A. Almoalem, I. Feldman, A. Lee, A. Kanigel, and G. Blumberg, *Superconductivity and Phonon Self-Energy Effects in Fe_{1+y}Te_{0.6}Se_{0.4}*, *Phys. Rev. Res.* **2**, 013373 (2020).
- [27] K. Ishida, Y. Onishi, M. Tsujii, K. Mukasa, M. Qiu, M. Saito, Y. Sugimura, K. Matsuura, Y. Mizukami, K. Hashimoto, and T. Shibauchi, *Pure Nematic Quantum Critical Point Accompanied by a Superconducting Dome*, *Proc. Natl. Acad. Sci. U.S.A.* **119**, e2110501119 (2022).
- [28] H.-H. Kuo, J.-H. Chu, J. C. Palmstrom, S. A. Kivelson, and I. R. Fisher, *Ubiquitous Signatures of Nematic Quantum Criticality in Optimally Doped Fe-Based Superconductors*, *Science* **352**, 958 (2016).
- [29] Q. Jiang, Y. Shi, M. H. Christensen, J. Sanchez, B. Huang, Z. Lin, Z. Liu, P. Malinowski, X. Xu, R. M. Fernandes, and J.-H. Chu, *Nematic Fluctuations in an Orbital Selective Superconductor Fe_{1+y}Te_{1-x}Se_x*, *arXiv:2006.15887*.
- [30] T. Watanabe, T. Otsuka, S. Hagiwara, Y. Koshika, S. Adachi, T. Usui, N. Sasaki, S. Sasaki, S. Yamaguchi, Y. Uezono, Y. Nakanishi, M. Yoshizawa, and S. Kimura, *Electronic Phase Diagram of Fe_{1+y}Te_{1-x}Se_x Revealed by Magnetotransport Measurements*, *Mod. Phys. Lett. B* **34**, 2040051 (2020).
- [31] Y. Sun, Z. Shi, and T. Tamegai, *Review of Annealing Effects and Superconductivity in Fe_{1+y}Te_{1-x}Se_x Superconductors*, *Supercond. Sci. Technol.* **32**, 103001 (2019).
- [32] See Supplemental Material at <http://link.aps.org/supplemental/10.1103/PhysRevX.13.011032> for the full datasets of magnetoresistance and TDO measurements, and details on the analysis of the upper critical field.
- [33] D. Braithwaite, G. Lapertot, W. Knafo, and I. Sheikin, *Evidence for Anisotropic Vortex Dynamics and Pauli Limitation in the Upper Critical Field of FeSe_{1-x}Te_x*, *J. Phys. Soc. Jpn.* **79**, 053703 (2010).
- [34] S. Khim, J. W. Kim, E. S. Choi, Y. Bang, M. Nohara, H. Takagi, and K. H. Kim, *Evidence for Dominant Pauli Paramagnetic Effect in the Upper Critical Field of Single-Crystalline FeTe_{0.6}Se_{0.4}*, *Phys. Rev. B* **81**, 184511 (2010).
- [35] S. Licciardello, N. Maksimovic, J. Ayres, J. Buhot, M. Čulo, B. Bryant, S. Kasahara, Y. Matsuda, T. Shibauchi, V. Nagarajan, J. G. Analytis, and N. E. Hussey, *Coexistence of Orbital and Quantum Critical Magnetoresistance in FeSe_{1-x}S_x*, *Phys. Rev. Res.* **1**, 023011 (2019).
- [36] M. Čulo *et al.* (unpublished).
- [37] Q. Wang, Y. Shen, B. Pan, Y. Hao, M. Ma, F. Zhou, P. Steffens, K. Schmalzl, T. R. Forrest, M. Abdel-Hafiez, X. Chen, D. A. Chareev, A. N. Vasiliev, P. Bourges, Y. Sidis, H. Cao, and J. Zhao, *Strong Interplay between Stripe Spin Fluctuations, Nematicity and Superconductivity in FeSe*, *Nat. Mater.* **15**, 159 (2016).
- [38] D. Arčon, P. Jeglič, A. Zorko, A. Potočnik, A. Y. Ganin, Y. Takabayashi, M. J. Rosseinsky, and K. Prassides, *Coexistence of Localized and Itinerant Electronic States in the Multiband Iron-Based Superconductor FeSe_{0.42}Te_{0.58}*, *Phys. Rev. B* **82**, 140508(R) (2010).
- [39] T. J. Liu, J. Hu, B. Qian, D. Fobes, Z. Q. Mao, W. Bao, M. Reehuis, S. A. J. Kimber, K. Prokeš, S. Matas, D. N. Argyriou, A. Hiess, A. Rotaru, H. Pham, L. Spinu, Y. Qiu, V. Thampy, A. T. Savici, J. A. Rodriguez, and C. Broholm, *From (π,0) Magnetic Order to Superconductivity with (π,π) Magnetic Resonance in Fe_{1.02}Te_{1-x}Se_x*, *Nat. Mater.* **9**, 718 (2010).
- [40] J. A. W. Straquadine, J. C. Palmstrom, P. Walmsley, A. T. Hristov, F. Weickert, F. F. Balakirev, M. Jaime, R. McDonald, and I. R. Fisher, *Growth of Nematic Susceptibility in the Field-Induced Normal State of an Iron-Based Superconductor Revealed by Elastoresistivity Measurements in a 65 T Pulsed Magnet*, *Phys. Rev. B* **100**, 125147 (2019).
- [41] T. Hanaguri, S. Niitaka, K. Kuroki, and H. Takagi, *Unconventional s-Wave Superconductivity in Fe(Se, Te)*, *Science* **328**, 474 (2010).
- [42] T. Hanaguri, K. Iwaya, Y. Kohsaka, T. Machida, T. Watashige, S. Kasahara, T. Shibauchi, and Y. Matsuda, *Two Distinct Superconducting Pairing States Divided by the Nematic End Point in FeSe_{1-x}S_x*, *Sci. Adv.* **4**, eaar6419 (2018).
- [43] J. L. Her, Y. Kohama, Y. H. Matsuda, K. Kindo, W. H. Yang, D. A. Chareev, E. S. Mitrofanova, O. S. Volkova, A. N. Vasiliev, and J. Y. Lin, *Anisotropy in the Upper Critical Field of FeSe and FeSe_{0.33}Te_{0.67} Single Crystals*, *Supercond. Sci. Technol.* **28**, 045013 (2015).

- [44] E. Helfand and N. R. Werthamer, *Temperature and Purity Dependence of the Superconducting Critical Field, H_{c2} . II*, *Phys. Rev.* **147**, 288 (1966).
- [45] A. I. Coldea, D. Braithwaite, and A. Carrington, *Iron-Based Superconductors in High Magnetic Fields*, *C. R. Phys.* **14**, 94 (2013).
- [46] S. Khim, B. Lee, J. W. Kim, E. S. Choi, G. R. Stewart, and K. H. Kim, *Pauli-Limiting Effects in the Upper Critical Fields of a Clean LiFeAs Single Crystal*, *Phys. Rev. B* **84**, 104502 (2011).
- [47] S. Rinott, K. B. Chashka, A. Ribak, E. D. Rienks, A. Taleb-Ibrahimi, P. Le Fevre, F. Bertran, M. Randeria, and A. Kanigel, *Tuning across the BCS-BEC Crossover in the Multiband Superconductor $\text{Fe}_{1+y}\text{Se}_x\text{Te}_{1-x}$: An Angle-Resolved Photoemission Study*, *Sci. Adv.* **3**, e1602372 (2017).
- [48] L. Wang, F. Hardy, T. Wolf, P. Adelman, R. Fromknecht, P. Schweiss, and C. Meingast, *Superconductivity-Enhanced Nematicity and ‘s + d’ gap symmetry in $\text{Fe}(\text{Se}_{1-x}\text{S}_x)$* , *Phys. Status Solidi B* **254**, 1600153 (2017).
- [49] D. Labat, P. Kotetes, B. M. Andersen, and I. Paul, *Variation of Shear Moduli across Superconducting Phase Transitions*, *Phys. Rev. B* **101**, 144502 (2020).
- [50] S. Nandi, M. G. Kim, A. Kreyssig, R. M. Fernandes, D. K. Pratt, A. Thaler, N. Ni, S. L. Bud’ko, P. C. Canfield, J. Schmalian, R. J. McQueeney, and A. I. Goldman, *Anomalous Suppression of the Orthorhombic Lattice Distortion in Superconducting $\text{Ba}(\text{Fe}_{1-x}\text{Co}_x)_2\text{As}_2$ Single Crystals*, *Phys. Rev. Lett.* **104**, 057006 (2010).
- [51] M. Yoshizawa, D. Kimura, T. Chiba, S. Simayi, Y. Nakanishi, K. Kihou, C.-H. Lee, A. Iyo, H. Eisaki, M. Nakajima, and S.-i. Uchida, *Structural Quantum Criticality and Superconductivity in Iron-Based Superconductor $\text{Ba}(\text{Fe}_{1-x}\text{Co}_x)_2\text{As}_2$* , *J. Phys. Soc. Jpn.* **81**, 024604 (2012).
- [52] Z. P. Yin, K. Haule, and G. Kotliar, *Kinetic Frustration and the Nature of the Magnetic and Paramagnetic States in Iron Pnictides and Iron Chalcogenides*, *Nat. Mater.* **10**, 932 (2011).
- [53] A. J. Millis, S. Sachdev, and C. M. Varma, *Inelastic Scattering and Pair Breaking in Anisotropic and Isotropic Superconductors*, *Phys. Rev. B* **37**, 4975 (1988).
- [54] Z. K. Liu, M. Yi, Y. Zhang, J. Hu, R. Yu, J. X. Zhu, R. H. He, Y. L. Chen, M. Hashimoto, R. G. Moore, S. K. Mo, Z. Hussain, Q. Si, Z. Q. Mao, D. H. Lu, and Z. X. Shen, *Experimental Observation of Incoherent-Coherent Crossover and Orbital-Dependent Band Renormalization in Iron Chalcogenide Superconductors*, *Phys. Rev. B* **92**, 235138 (2015).
- [55] I. Paul and M. Garst, *Lattice Effects on Nematic Quantum Criticality in Metals*, *Phys. Rev. Lett.* **118**, 227601 (2017).
- [56] A. I. Coldea, S. F. Blake, S. Kasahara, A. A. Haghighirad, M. D. Watson, W. Knafo, E. S. Choi, A. McCollam, P. Reiss, T. Yamashita, M. Bruma, S. C. Speller, Y. Matsuda, T. Wolf, T. Shibauchi, and A. J. Schofield, *Evolution of the Low-Temperature Fermi Surface of Superconducting $\text{FeSe}_{1-x}\text{S}_x$ across a Nematic Phase Transition*, *npj Quantum Mater.* **4**, 2 (2019).
- [57] S. Licciardello, J. Buhot, J. Lu, J. Ayres, S. Kasahara, Y. Matsuda, T. Shibauchi, and N. E. Hussey, *Electrical Resistivity across a Nematic Quantum Critical Point*, *Nature (London)* **567**, 213 (2019).
- [58] W. K. Huang, S. Hosoi, M. Čulo, S. Kasahara, Y. Sato, K. Matsuura, Y. Mizukami, M. Berben, N. E. Hussey, H. Kontani, T. Shibauchi, and Y. Matsuda, *Non-Fermi Liquid Transport in the Vicinity of the Nematic Quantum Critical Point of Superconducting $\text{FeSe}_{1-x}\text{S}_x$* , *Phys. Rev. Res.* **2**, 033367 (2020).
- [59] M. Bristow, P. Reiss, A. A. Haghighirad, Z. Zajicek, S. J. Singh, T. Wolf, D. Graf, W. Knafo, A. McCollam, and A. I. Coldea, *Anomalous High-Magnetic Field Electronic State of the Nematic Superconductors $\text{FeSe}_{1-x}\text{S}_x$* , *Phys. Rev. Res.* **2**, 013309 (2020).
- [60] D. Labat and I. Paul, *Pairing Instability near a Lattice-Influenced Nematic Quantum Critical Point*, *Phys. Rev. B* **96**, 195146 (2017).
- [61] G. Grissonnanche *et al.*, *Direct Measurement of the Upper Critical Field in Cuprate Superconductors*, *Nat. Commun.* **5**, 3280 (2014).
- [62] B. J. Ramshaw, S. E. Sebastian, R. D. McDonald, J. Day, B. S. Tan, Z. Zhu, J. B. Betts, R. Liang, D. A. Bonn, W. N. Hardy, and N. Harrison, *Quasiparticle Mass Enhancement Approaching Optimal Doping in a High- T_c Superconductor*, *Science* **348**, 317 (2015).
- [63] M. K. Chan, R. D. McDonald, B. J. Ramshaw, J. B. Betts, A. Shekhter, E. D. Bauer, and N. Harrison, *Extent of Fermi-Surface Reconstruction in the High-Temperature Superconductor $\text{HgBa}_2\text{CuO}_{4+\delta}$* , *Proc. Natl. Acad. Sci. U.S.A.* **117**, 9782 (2020).
- [64] H. Q. Yuan, F. M. Grosche, M. Deppe, C. Geibel, G. Sparn, and F. Steglich, *Observation of Two Distinct Superconducting Phases in CeCu_2Si_2* , *Science* **302**, 2104 (2003).
- [65] D. Leboeuf, N. Doiron-Leyraud, J. Levallois, R. Daou, J. B. Bonnemaïson, N. E. Hussey, L. Balicas, B. J. Ramshaw, R. Liang, D. A. Bonn, W. N. Hardy, S. Adachi, C. Proust, and L. Taillefer, *Electron Pockets in the Fermi Surface of Hole-Doped High- T_c Superconductors*, *Nature (London)* **450**, 533 (2007).
- [66] N. Doiron-Leyraud, C. Proust, D. Leboeuf, J. Levallois, J.-B. Bonnemaïson, R. Liang, D. A. Bonn, W. N. Hardy, and L. Taillefer, *Quantum Oscillations and the Fermi Surface in an Underdoped High- T_c Superconductor*, *Nature (London)* **447**, 565 (2007).
- [67] J. Chang, E. Blackburn, A. T. Holmes, N. B. Christensen, J. Larsen, J. Mesot, R. Liang, D. A. Bonn, W. N. Hardy, A. Watenphul, M. V. Zimmermann, E. M. Forgan, and S. M. Hayden, *Direct Observation of Competition between Superconductivity and Charge Density Wave Order in $\text{YBa}_2\text{Cu}_3\text{O}_{6.67}$* , *Nat. Phys.* **8**, 871 (2012).